Egypt. J. Chem. **Vol. 64,** No. 3 pp. 1197 - 1205 (2021)

Egyptian Journal of Chemistry

http://ejchem.journals.ekb.eg/

Application of Cs/ZnO/GO Hybrid Nanocomposite for Enhanced Inter-behavior of Electronic Properties and Thermal Stability as Corrosion Inhibitor

Hend A. Ezzat,[a*], Maroof A. Hegazy,[a], Nadra A. Nada,[b], Osama Osman,[c], Medhat A. Ibrahim[c]

[a]*Nano Technology Unit, Solar and Space Research Department, National Research Institute of Astronomy and Geophysics (Nano NRIAG), 11421 Helwan, Cairo, Egypt*

[b]*Physics Department, Faculty of Women for Arts, Science and Education, Ain Shams University, 11757 Cairo, Egypt*

[c]*Molecular Spectroscopy and Modeling Unit, Spectroscopy Department, National Research Centre, 33 El-Bohouth St., 12622, Dokki, Giza, Egypt*

Abstract

Polymer hybrid nanocomposites are considered to be one of the most promising materials which in turn acquires new, multiple and improved properties such as optical properties and electrical conductivity used for various applications in the fields of optical integrated circuits, sensors, adhesives, coatings and corrosion inhibitors for metal protection. At the present time graphene oxide hybridization with metal oxide modified carbohydrate polymers performance for corrosion inhibition for metal. Hybrid nanocomposite Cs/ZnO/GO was considered to be studied by DFT theory. The considered Cs/ZnO/GO model structure were studied in the two interaction states once as adsorb state and once as complex state. Hybrid nanocomposite electronic properties and thermal stability in all designated states have been evaluated. B3LYP/LANL2DZ was used to calculate TDM, HOMO/LUMO band gap energy and MESP for hybrid Cs/ZnO/GO nano composite assumptions. Additionally, QSAR descriptors for thermal stability study were also calculated for the same interactions. The most certainly stable structure of the hybrid nanocomposite Cs/ZnO/GO was found to occur through OH of the carboxyl group COOH of GO in complex mechanism and through O of the carboxyl group COOH of GO in adsorb mechanism. It is also found that the structure Cs/ZnO/GO occurs by O of the carboxyl group COOH of GO in adsorb mechanism has a significant improvement in electronic properties and thermal stability with band gap 0.1750 eV that it could be used as Corrosion Inhibitor.

Keywords: Chitosan; Graphene Oxide; ZnO; Hybrid nanocomposites; MESP; QSAR.

1. Introduction

Naturally biopolymers are a kind of materials as results of biochemical processes in living organisms, which have been used for different material applications; as binders, drug delivery, coatings and corrosion inhibitors [1-3]. There are also several green and safe carbohydrate biopolymers and their derivatives used to prevent metal corrosion. Protection mechanisms directly correlated to their chemical composition, macromolecular weights, and there specific molecular and electronic structures [4-6]. Many of the pure or modified carbohydrate polymers investigated that their grafted structures and nanoparticle composites with a multitude of potentials were applied for applications of metal protection [7-9]. Polymer hybrid nanocomposites are a promising new material with better optical properties and electrical conductivity used in various applications in the fields of medicine, drug delivery, microelectronic packaging, packaging materials, optical integrated circuits, sensors, coatings and adhesives [10,11]. Generally, the hybridization strategy has successfully promoted grapheme oxide (GO) corrosion inhibition performance [12]. Moreover, modification with GO was used for aircraft structure compound coatings as corrosion inhibiting [13]. GO was presented by using sol-gel method to enhance the film obtained from AA2024-T3 aluminum alloys corrosion protection properties [14]. The GO/ZnO composite is known as a successful candidate for energy storage applications according to have high dielectric permittivity and low tangent loss values [15]. New perspective of graphene

*Corresponding author e-mail: hend_ahmed16@yahoo.com.; (Hend A. Ezzat).
Receive Date: 30 December 2020, Accept Date: 15 January 2021
DOI: 10.21608/EJCHEM.2021.55872.3188

and chitosan matrix composite with innovative electrical, optical and stability properties were obtained which could be applied in various advanced applications [16]. Furthermore, graphene oxide/chitosan/zinc oxide (GO/Cs/ZnO) ternary nano-hybrids was synthesized and characterized by Langmuir isotherm used in three methods (PDP, EIS and LPR) to study the adsorption of nano-materials on mild steel [17]. Hybrid composite of Cs/ZnO/GO register significant enhancement for the thermal and mechanical properties [18]. Low cost CH/GO/ZnO/PANI hybrid nanocomposites demonstrate strong super-capacity efficiency and long-term cycle stability. Such findings demonstrate the promise of hybrid nanocomposites as high-performance supercapacitors [19]. As well, hybrid with other nano metal oxides make a significant enhancement as, the measurements of electrochemical impedance studies (EIS) and potentiodynamic polarization (PP) revealed that the chitosan-doped-Hybrid/nano-TiO2 sol-gel coating provided greater safety against corrosion than the undoped hybrid/TiO2 nanocomposite coating [20]. Molecular modeling is a theoretical simulation using molecular dynamics, which is an important method for the study of chemical structures, particularly nanomaterials [21-27]. The studies of the chemical, physical and electronic properties of many structures were performed using various levels of molecular modeling theories [28-34]. It is important to study polymeric systems as synthetic and/or natural and their polymer nanocomposite matrices using molecular modeling such as HOMO/LUMO bandgap energy, total dipole moment (TDM) and molecular electrostatic potential (MESP) [35-39]. Physical and electronic properties may be used to determine the reactivity of the system under consideration [40-44]. Also, according quantum mechanics, quantitative structure analysis relationship (QSAR) is another computational method used to analyze the molecular behavior that is consistent with molecular modeling. Calculations of QSAR are used to analyze the biological behavior and physicochemical properties of chemical molecules used in electronics, chemical and biological sciences [45-50]. The QSAR descriptors included in calculations give specific properties as structural, chemical and physical properties for the molecules studied. In relation, there are a number of important descriptors, including those defining the electronic effects within molecules of lipophilicity [51].

So that, density functional theory (DFT) calculations were conducted to evaluate the electronic properties and thermal stability of the Hybrid nano composite Cs/ZnO/GO. Through these Cs structures interacted as hybridization with ZnO and GO in the state of adsorption and complex interactions, HOMO/LUMO band gap energy (ΔE), total dipole moment (TDM) and molecular electrostatic potential (MESP) were calculated at B3LYP/LANL2DZ. The some QSAR descriptors were also calculated for the same interactions.

2. Computational Details

Hypothesized structures representing Cs interacted as hybridization with ZnO and GO in the state of adsorb and complex interactions were conducted to DFT calculations at B3LYP level with LANL2DZ basis set. All postulate models were conducted to study the electronic properties by calculating the HOMO/LUMO bandgap energy (ΔE) and TDM. Furthermore, MESP of all assumed structures were studied via same theory of calculations. QSAR descriptors were calculated for structures at PM6 level. All models based on programs performed at Spectroscopy Department, National Research Centre, NRC.

3. Results and Discussion

Hybrid nanocomposites of natural polymer (NP) described by Cs to analyze transformations occurring in the electronic properties of NP in the presence of metal oxides (MO) and graphene GO. Postulated mechanisms were classified into two classes. First mechanism supposed to represent adsorption interaction Cs with ZnO and GO adsorption hybrid composite. Three unit of Cs with ZnO and GO adsorption hybrid composite mechanism was divided into four position of interaction according to the functional groups of GO which are O, OH and carboxyl (COOH) group. The four interactions positions were assumed as Cs/ZnO/GO interacted through O atom bridge (P1), Cs/ZnO/GO interacted through OH group (P2), Cs/ZnO/GO interacted through OH of COOH group (P3) and Cs/ZnO/GO interacted through C=O of COOH group (P4). Second mechanism represent complex assumption of Cs interaction with ZnO and GO hybrid composite. Electronic properties for both mechanisms were investigated by calculating TDM and HOMO/LUMO band gap energy at the same theoretical level. DFT was used for postulated structures at B3LYP level with LANL2DZ basis set. Optimized structures of base material configuration and HOMO/LUMO band gap energy for Cs and GO demonstrating in figure 1. Tables 1 demonstrate the values of TDM and the energy difference of HOMO/LUMO bands of the Cs and GO based materials. Cs and GO TDM values were registered as 4.094 and 14.1457 Debye, and 2.571 and 0.5214 eV were registered for Cs and GO band gap energy.

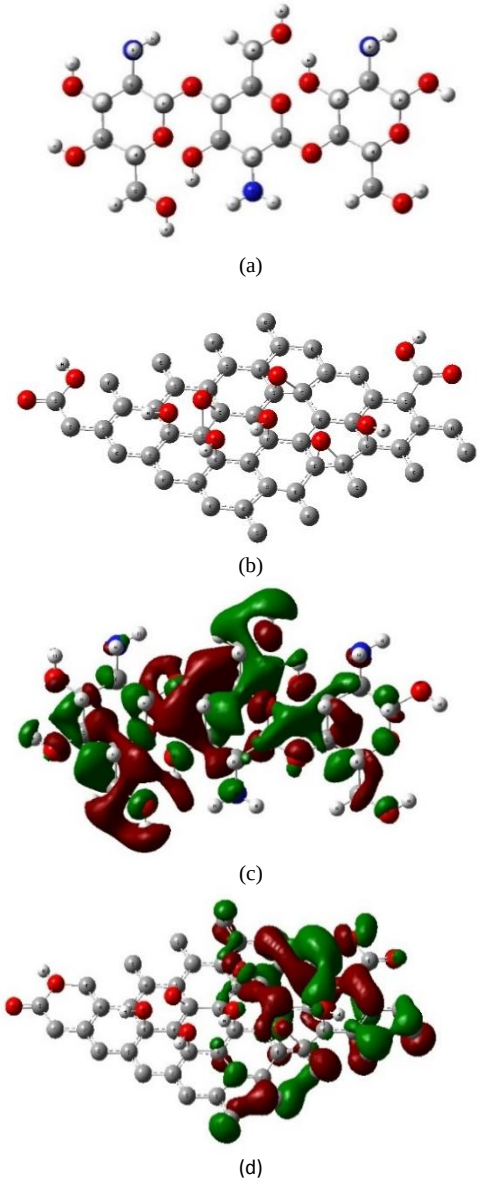

Fig. 1. Optimized structure of (a) Chitosan (b) Graphene Oxide base materials and HOMO/LUMO band gap energy for (c) Chitosan (d) Graphene Oxide base materials

Table 1. Optimized TDM (Debye) and HOMO/LUMO band gap energy ΔE (eV) Using B3LYP/LANL2DZ for Cs and GO

Structure	TDM	ΔE
Cs	4.094	2.571
GO	14.1457	0.5214

3.1. Cs/ ZnO /GO adsorb mechanism

The first system is designed to reflect adsorption interaction Cs with ZnO and GO hybrid composite adsorption. Hybrid composite Cs with ZnO and GO adsorption system is categorized into four interaction positions according to the GO active groups as O, OH and carboxyl (COOH) groups. The four contact positions is considered as Cs/ZnO/GO interacted through O atom bridge (P1), Cs/ZnO/GO interacted through OH group (P2), Cs/ZnO/GO interacted through OH of COOH group (P3) and Cs/ZnO/GO interacted through C=O of COOH group (P4) as adsorb state. Optimized model and the energy gap of HOMO/LUMO bands for supposing adsorb mechanism structures illustrated in figure 2. Table 2 represented the adsorb mechanism of TDM and HOMO/LUMO band gap energy variability. In the case of Cs/ZnO/GO (P1) the TDM increased to 54.7155 Debye, while the band gap ΔE decreased to 0.278 eV. In Cs/ZnO/GO (P2) and Cs/ZnO/GO (P3) it was observed that TDM had significantly improved to 63.7060 and 79.8792 Debye and the band gap had significantly reduced to 0.1780 and 0.1750 eV, but for Cs/ZnO/GO (P4) TDM had also changed to 78.3511 Debye and band gap ΔE had also changed to 0.2808 eV. A substantial increase in electrical properties was reported from all data on the adsorb mechanism Cs/ZnO/GO interacted via the COOH group (P3) OH.

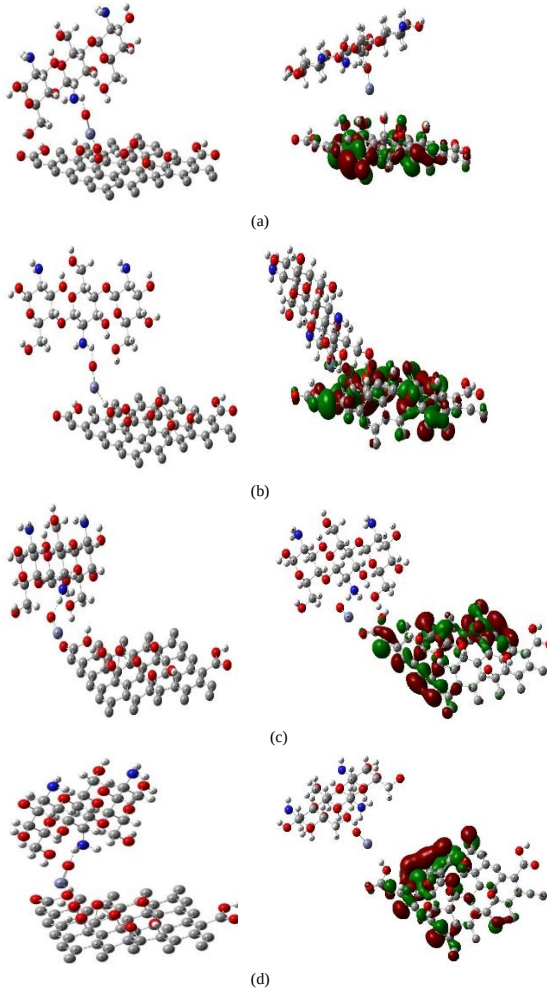

Fig. 2. Optimized structures of hybrid composite Cs with ZnO and GO adsorb mechanism of interaction and HOMO/LUMO band gap energy as (a) Cs/ZnO/ GO (P1) (b) Cs/ZnO/ GO (P2) (c) Cs/ZnO/ GO (P3) (d) Cs/ZnO/ GO (P4)

Table 2. Optimized TDM (Debye) and HOMO/LUMO band gap energy ΔE (eV) Using B3LYP/LANL2DZ for hybrid composite Cs with ZnO and GO adsorb mechanism of interaction

Structure	TDM	ΔE
CS /ZnO/ GO (P1)	54.7155	0.3380
CS /ZnO/ GO (P2)	63.7060	0.1780
CS /ZnO/ GO (P3)	79.8792	0.1750
CS /ZnO/ GO (P4)	78.3511	0.2808

3.2. Cs/ZnO/GO complex mechanism

The second method is planned to model the complex interaction between the ZnO and GO hybrid nanocomposite Cs. As described above, complex structures are often divided into four GO active group interaction positions such as O, OH and Carboxyl (COOH) groups. The four dominant positions are known to be Cs/ZnO/GO interacted through O atom bridge (P1), Cs/ZnO/GO interacted through OH group (P2), Cs/ZnO/ GO interacted through C= O of COOH group (P3) and Cs/ZnO/GO interacted through OH of COOH group (P4) as complex state. Figure 3 demonstrated Optimized estimation of complex mechanism structures and energy gap for HOMO/LUMO bands. Table 3 was the complex mechanism of the TDM and the HOMO/LUMO band of energy variation differences Cs/ZnO/GO (P1) The TDM improved to 35.0208 Debye, while the band gap ΔE decreased to 0.2346 eV. In Cs/ZnO/GO (P2) and Cs/ZnO/GO (P3) it was found that the TDM increased to 34.1965 and 74.3220 Debye and the band gap decreased to 0.2887 and 0.4504 eV, but the Cs/ZnO/GO (P4) TDM had also changed to 73.0965 Debye and the band gap ΔE had also changed to 0.2465 eV. In a complex system, the position Cs/ZnO/GO interacted through OH of the COOH group (P4) reported the most electrical improvement properties.

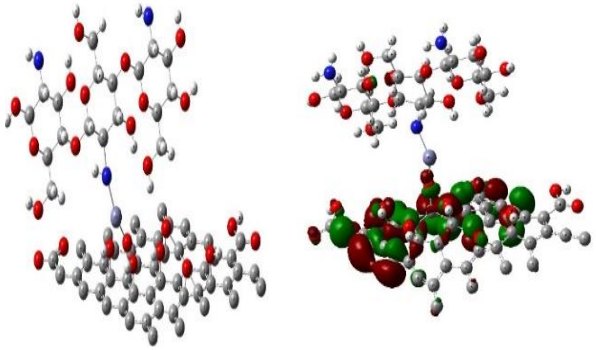

(a)

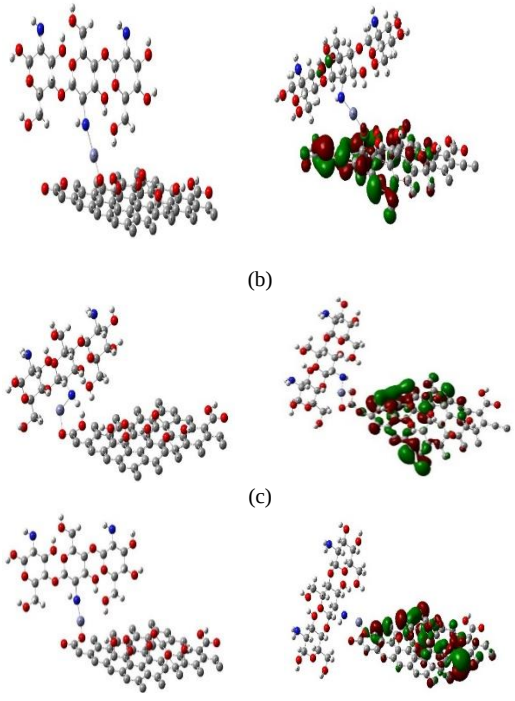

(b) (c) (d)

Fig. 3. Optimized structures of hybrid composite Cs with ZnO and GO complex mechanism of interaction and HOMO/LUMO band gap energy as
(a) Cs /ZnO/ GO (P1) (b) Cs /ZnO /GO (P2)
(c) Cs /ZnO/ GO (P3) (d) Cs /ZnO/ GO (P4)

Table 3. Optimized TDM (Debye) and HOMO/LUMO band gap energy ΔE (eV) Using B3LYP/LANL2DZ for hybrid composite Cs with ZnO and GO complex mechanism of interaction

Structure	TDM	ΔE
CS /ZnO/ GO (P1)	35.0208	0.2346
CS /ZnO/ GO (P2)	34.1965	0.2887
CS /ZnO/ GO (P3)	74.3220	0.4504
CS /ZnO/ GO (P4)	73.0965	0.2465

3.3. Molecular Electrostatic Potential (MESP):

To define the reactivity and stability of hybrid composite Cs with ZnO and GO in the two postulate mechanisms, MESP was also determined for them. The importance of MESP is due to its potential in linking the results of the total charge distribution with electronegativity, dipole moment, partial charges and site of chemical reactivity of a molecule. MESP is a significant parameter that gives information about the nuclear and electronic charge distribution of molecule, as well as being a method for understanding and predicting chemical reactivity. Correspondingly, MESP is a visual tool for understanding the relative polarity of a molecule and acts as a useful quantity to illustrate the relationship of hydrogen bonding, reactivity, and structure-activity of the interacting molecules. So, MESP was calculated for the two proposed mechanisms of hybrid composite Cs with ZnO and GO to explore molecular reactivity by

evaluating active sites and nucleophilic or electrophilic properties of molecules under investigation. Given the fact that the distribution of the molecular charge remains undisturbed, the electrostatic potential of the molecule is still a strong guide in determining the reactivity of the molecules against positive or negatively charged reactants. Specific values of the electrostatic potential appear on the surface of the molecule in various colors. Electron density values rise in the following order: Red > Orange > Yellow > Green > Blue. Generally, the attractive potential occurs in red colored areas, and the repulsive potential occurs in blue. In the MESP surface, the color variation defined as red refers to the electron-rich (negative) region, the blue color refers to the electron-poor (positive) region, and the green color indicates zero electrostatic potential. The MESP at various points on the electron density isosurface of based materials and the two suggested hybrid composite Cs mechanisms with ZnO and GO is shown by the color isosurface in figure 4, 5 and 6.

MESP isosurface of hybrid composite Cs structures with ZnO and GO clearly shows that there are no negative MESP regions found on the isosurface where only positive MESP regions are found. Furthermore, it is clear that the highest positive area is often located on the Cs surface, which is known to be suitable for nucleophilic attacks. The findings obtained from MESP showed that these structures were extremely stable and that the MESP isosurface was observed in blue and yellow colors.

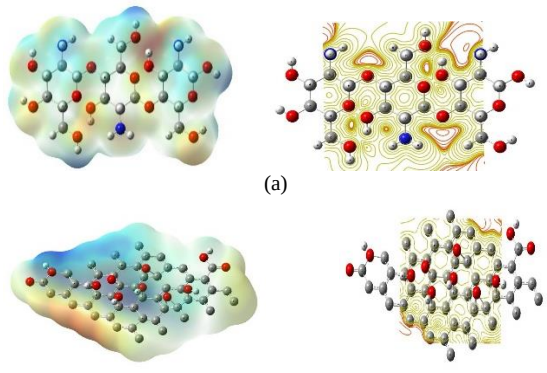

(a)

(b)

Fig. 4: MESP of base materials as (a) Chitosan (b) Graphene Oxide

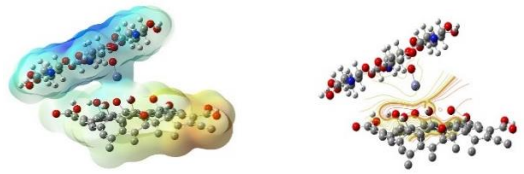

(a)

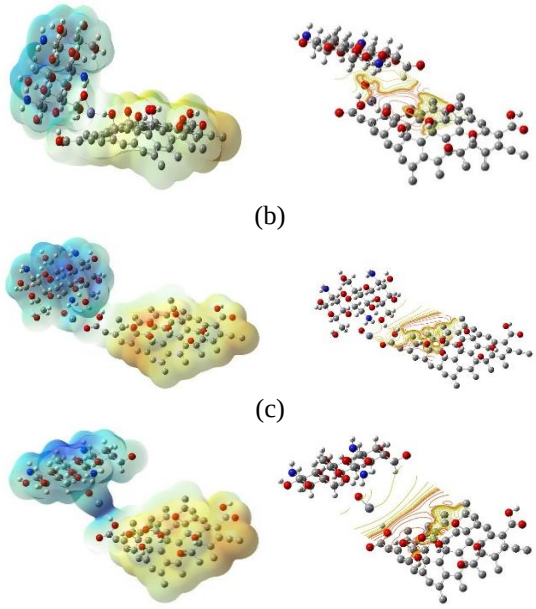

(b)

(c)

(d)

Fig. 5. MESP of hybrid composite Cs with ZnO and GO adsorb mechanism of interaction as total density mapped surface and contour as (a) CS/ZnO/GO (P1), (b) CS/ZnO/GO (P2), (c) CS/ZnO/GO (P3) and (d) CS/ZnO/GO (P4).

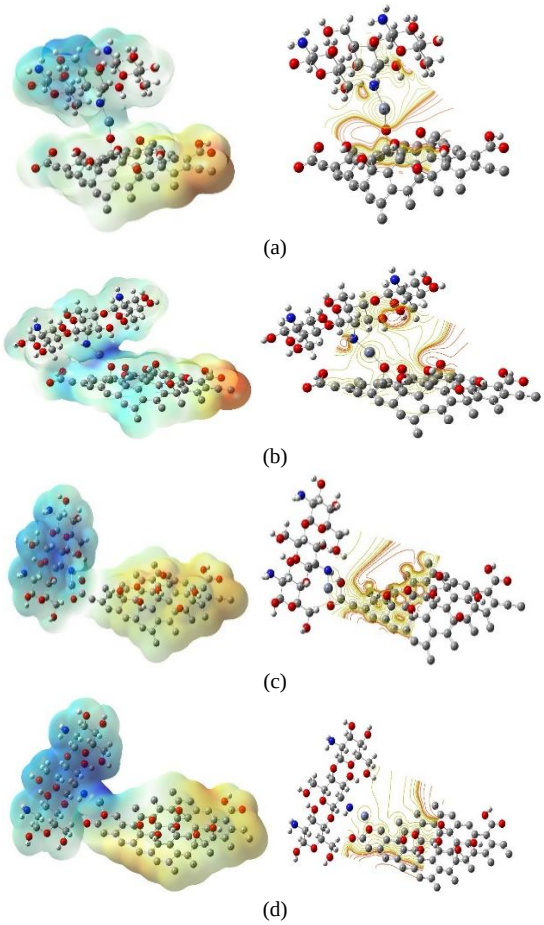

(a)

(b)

(c)

(d)

Fig. 6. MESP of hybrid composite Cs with ZnO and GO complex mechanism of interaction as total density mapped surface and contour as (a)CS/ZnO/GO (P1), (b) CS/ZnO/GO (P2), (c)CS/ZnO/GO (P3) and (d) CS/ZnO/GO (P4)

3.4. QSAR descriptors

QSAR descriptors were determined for Cs and GO as based materials and hybrid composite Cs with ZnO and GO mechanisms. QSAR descriptors are shown in table 4 as charge, total energy (TE), heat formation (HF), ionization potential (IP), log P, polarization, molar refractive (MR), molecular weight (MW), surface area and volume.

The first descriptor charge was equal to zero that the postulate structures were in the ground state. The total energy descriptor (TE) was then calculated to characterize the stability of the system, and when the TE decreases the structure defined as more stable. As shown in Table 4 TE, Cs and GO for base materials were equivalent to -8479.409 and -11314.284 eV, respectively. TE reported improved in hybrid composite Cs with ZnO and GO adsorb mechanism that TE for Cs/ZnO/GO (P1), Cs/ZnO/GO (P2), Cs/ZnO/GO (P3) and Cs/ZnO/GO (P4) were 18889.308,-20188.437,-20206.621 and -20199.602 eV which indicated that the most stable structure were Cs/ZnO/GO (P3) and Cs/ZnO/GO (P4). Similarly, for hybrid composite Cs with ZnO and GO complex mechanism for Cs/ZnO/GO (P4), TE makes the shift only equal to -20518.366, which reflects a more stable structure.

HF is a vital thermal descriptor that defines the energy produced as heat, as atoms reside at potentially infinite distances, link and create a molecule. Far as the HF is concerned, it can be defined as a shift in the enthalpy after the formation of a single mole of a substance from its components in its natural and stable state under atmospheric standard conditions at a given temperature. The amount of heat produced or absorbed into a single mole is specified for the heat of the material, for a particular substance. Table 4 shows that the lowest HF values in the two interaction mechanisms were Cs/ZnO/GO (P4) and Cs/ZnO/GO (P4) for adsorb and complex, respectively, which reported a minimum amount of energy to be generated.

The significant QSAR descriptor is the IP that characterizes the reactivity of the compound. IP is defined as the energy needed for the compound to be ionized. The IP value decreases, as the reactivity of chemical compounds increase. The data reflected that the two mechanisms did not show a substantial difference in the IP. The highest IP values were -9.191 and -9.264 for Cs/ZnO/GO (P1) adsorb and Cs/ZnO/GO (P3) complex mechanism, while the lowest IP values were -8.765 and -7.992 for Cs/ZnO/GO (P3) adsorb and Cs/ZnO/GO (P4) complex mechanism respectively.

The logarithm of the partition coefficient (log P) is the descriptor describing the hydrophilicity of the chemical product. Log P is equivalent to the amount of dissolving material in organic solution for dissolving in aqueous solvents. Consequently, positive log P values are related to hydrophobic compounds and negative values are indicated for hydrophilic compounds. Both mechanisms have a negative log P under which the substances are hydrophilic (water soluble).

Polarizability can be defined as a simple property which describes how the chemical structure can be polarized in response to external forces that represent the reactivity of the chemical structures, which depends on their volume. The model structures contribute to a large increase in polarizability. In fact, the molar refractor is a descriptor that determines the total polarization of the mole of the material. The higher the molar refractive, the greater the reactivity of structures. As defined in Table 4 Cs/ZnO/GO (P3) and Cs/ZnO/GO (P4) for adsorb mechanism and Cs/ZnO/GO (P4) for complex mechanism, more reactive structures have been reported.

The surface area and volume are both physical parameters of the QSAR. As specified in Table 4 Cs/ZnO/GO (P4) for the adsorb mechanism and Cs/ZnO/GO (P4) for the complex mechanism of high surface area and volume as 1019.720, 1052.190, 942.100 and 993.12.

Such findings make the supposed Cs/ZnO/GO (P4) for the adsorb mechanism and Cs/ZnO/GO (P4) for the complex mechanism structure a promising new material with an efficient cost, more durable (physically and chemically), thermally stable and more sensitive.

Table 4. QSAR descriptors using semiempirical theory at PM6 level as Charge, Total Energy(ev), Heat of formation (HF), Ionization potential (eV), Log P, Polarizability, Molar refractive (MR), molecular weight (MW), surface area and volume for hybrid composite Cs with ZnO and GO as adsorb state and complex state in the four positions of interaction

	Structure	Charge	T E (ev)	HF	IP(eV)	LogP	Polarizability	MR	MW	Surface Area	Volume
	Cs	0	-8479.409	-578.295	-9.720	-5.236	30.727	105.723	501.483	444.260	387.570
	GO	0	-11314.284	865.987	-9.199	-11.799	110.455	200.287	794.587	506.08	494.81
Adsorb	CS/ZnO/GO (P1)	0	18889.308	217.254	-9.191	-15.995	145.062	309.412	1377.478	969.430	904.980
Adsorb	CS/ZnO/GO (P2)	0	-20188.437	214.207	-8.797	-17.421	136.657	304.543	1377.478	989.030	932.290
Adsorb	CS/ZnO/GO (P3)	0	-20206.621	309.351	-8.765	-17.616	160.279	311.392	1377.478	1001.410	934.690
Adsorb	CS/ZnO/GO (P4)	0	-20199.602	184.012	-9.035	-15.659	144.187	310.077	1377.478	1019.720	942.100
Complex	CS/ZnO/GO (P1)	0	36740.705	612.387	-8.57	-14.807	158.207	296.413	1360.471	959.36	902.46
Complex	CS/ZnO/GO (P2)	0	37262.446	145.062	-8.635	-17.393	157.559	304.244	1359.463	959.020	902.9
Complex	CS/ZnO/GO (P3)	0	37412.860	306.412	-9.264	-16.502	149.293	301.787	1359.463	972.510	909.3
Complex	CS/ZnO/GO (P4)	0	-20518.366	-607.736	-7.992	-9.878	132.736	322.565	1387.685	1052.190	993.12

4. Conclusion:

DFT calculations were carried out to evaluate the effect of hybrid nanocomposite Cs/ZnO/GO on the electronic properties and thermal stability of certain NP polysaccharides. TDM, HOMO/LUMO bandgap energy and MESP were evaluated using B3LYP / LANL2DZ for all the assumed structure of hybrid nanocomposite Cs/ZnO/GO. For studying the chemical, physical and thermal stability, QSAR descriptors were calculated for the same interactions. Electronic properties reported a substantial increase in the development of the hybrid nanocomposite Cs / ZnO / GO was found to occur through the OH of the carboxyl group COOH of GO in a complex mechanism and through the O of the carboxyl group COOH of GO in an adsorbing mechanism with a band gap of 0.2465 and 0.1750 eV respectively.

Exponentially, the readings of QSAR, geometric and thermal properties confirmed that the hybridization of Cs / ZnO / GO physical, thermal stability and reactivity eventually lead to the new material structure has significant properties as an efficient cost, more stable (physically and chemically), thermally stable and more reactive, in particular the hybridization of Cs/ZnO/GO through the O of the carboxyl group COOH of GO in an adsorbing mechanism. Extracting TDM, band gap energy, MESP and QSAR descriptors it could be observed that the studied hybridization of Cs/ZnO/GO provides reasonable as corrosion inhibitor applications due to a combination of high carrier mobility, low responsiveness to the surrounding field and thermal stability. Hybrid nanocomposite Cs/ ZnO / GO is also an innovative new technology for a wide variety of uses, including coatings, electrical products, adhesives and optical circuits.

5. References

[1] Umoren S. A., Eduok U. M., Application of carbohydrate polymers as corrosion inhibitors for metal substrates in different media: A review, Carbohydrate Polymers, 140, 314-34 (2016).

[2] Charles A.B., Vacuum Deposition Onto Webs, Films, and Foils. William Andrew, Elsevier, 8155 (2007).

[3] DufresneA., Polysaccharide nano crystal reinforced nanocomposites, Canadian Journal of Chemistry, 86, 484-494 (2008).

[4] Ashrafi H., Azadi A., Chitosan-based hydrogel nanoparticle amazing behaviors during transmission electron microscopy, International Journal of Biological Macromolecules, 84, 31-34 (2015).

[5] Saboktakin M. R., Tabatabaie R. M., Maharramov A., Ramazanov M. A., Synthesis and characterization of pH-dependent glycol chitosan and dextran sulfate nanoparticles for effective brain cancer treatment, International Journal of Biological Macromolecules, 49, 747-751 (2011).

[6] Yu S., Xu X., Feng J., Liu M., Hu K., Chitosan and chitosan coating nanoparticles for the treatment of brain disease. International Journal of Pharmaceutics, 560, 282-293(2019).

[7] Rioux L. E., Turgeon S. L., Beaulieu M., Characterization of polysaccharides extracted from brown seaweeds, Carbohydrate Polymers, 69, 530-537 (2007).

[8] Gomez C. G., Pérez Lambrecht M. V., Lozano J. E., Rinaudo M., Villar M.A., Influence of the extraction–purification conditions on final properties of alginates obtained from brown algae (Macrocystis pyrifera), International Journal of Biological Macromolecules, 44, 365-371 (2009).

[9] Kovalenko I., Zdyrko B., Magasinski A., Hertzberg B., Milicev Z., A major constituent of brown algae for

use in high-capacity Li-Ion batteries, Science, 334, 75-79 (2011).

[10] Hashim A., Al-Attiyah Kh. H. H., Obaid S. F., Modern Developments of Polymer Blend/ Oxide Nanocomposites for Biomedical Applications as Antibacterial and Radiation Shielding Materials: A Review, Research Journal of Agriculture and Biological Sciences, 14(1), 8-18 (2019).

[11] Ezzat H. A., Hegazy M. A., Nada N. A., Osman O., Ibrahim M. A., Application of Natural Polymers Enhanced with ZnO and CuO as Humidity Sensor, NRIAG Journal of Astronomy and Geophysics, 9, 586-597(2020).

[12] Jena G., Anandkumar B.,Vanithakumari S.C.,George R.P., Philip J., Amarendra G., Graphene oxide-chitosan-silver composite coating on Cu-Ni alloy with enhanced anticorrosive and antibacterial properties suitable for marine applications, Progress in Organic Coatings, 139, 105444 (2020).

[13] Zhang H., Zhou H., Yang J., Song Y., Zhao L., Synergism of modified graphene oxide to aircraft structural corrosion inhibiting compounds coatings, Progress in Organic Coatings, 132, 490-498 (2019).

[14] Xue B., Yu M., Liu J., Liu J., Xiong L., Corrosion protection of AA2024-T3 by sol-gel film modified with graphene oxide, Journal of Alloys and Compounds, 725, 84-95 (2017).

[15] Mututu V., Sunitha A. K., Thomas R., Pandey M., Manoj B., An Investigation on Structural, Electrical and Optical properties of GO/ZnO Nanocomposite, International Journal of Electrochemical Science, 14, 3752 – 3763 (2019).

[16] Ozkana B. C., Sogancib T., Turhana H., Akb M., Investigation of rGO and chitosan effects on optical and electrical properties of the conductive polymers for advanced applications, Electrochimica Acta, 295, 1044-1051(2019).

[17] Majidi H. J., Mirzaee A., Jafari S. M., Amiri M., Shahrousvand M., Babaei A., Fabrication and characterization of graphene oxide-chitosan-zinc oxide ternary nano-hybrids for the corrosion inhibition of mild steel, International Journal of Biological Macromolecules, 148, 1190-1200 (2020).

[18] Sanmugam A., Vikraman Dh., Park H. J., Kim H.-S., One-Pot Facile Methodology to Synthesize Chitosan-ZnO-Graphene Oxide Hybrid Composites for Better Dye Adsorption and Antibacterial Activity, Nanomaterials (Basel), Nov; 7(11), 363 (2017).

[19] Anandhavelu S., Dhanasekaran V, Sethuraman V., Joon P. H., Chitin and Chitosan Based Hybrid Nanocomposites for Super Capacitor Applications, Journal of Nanoscience and Nanotechnology, 17(8), 1321-1328 (2017).

[20] Balaji J., Sethuraman M.G., Chitosan-doped-hybrid/TiO2 nanocomposite based sol-gel coating for the corrosion resistance of aluminum metal in 3.5% NaCl medium, International Journal of Biological Macromolecules, 104, 1730-1739 (2017).

[21] Bayoumy A.M., El-Sayed E.M., Omar A., Ibrahim M., Emerging Applications of Chitosan: From Biology to Environment. Biointerface Research in Applied Chemistry, 8, 3368–3380 (2018).

[22] Fahmy A., Khafagy R.M., Elhaes H., Ibrahim M. A., Molecular Properties of Polyvinyl Alcohol/Sodium Alginate Composite, Biointerface Research in Applied Chemistry, 10, 4734-4739 (2020).

[23] Ibrahim A., Elhaes H.; Meng F., Ibrahim M., Effect of Hydration on the Physical Properties of Glucose, Biointerface Research in Applied Chemistry, 8, 4114-4118 (2019).

[24] Abdel-Bary A.S., Tolan D.A., Nassar M.Y., Taketsugu T., El-Nahas A.M., Chitosan, magnetite, silicon dioxide, and graphene oxide nanocomposites: Synthesis, characterization, efficiency as cisplatin drug delivery, and DFT calculations. International Journal of Biological Macromolecules, 154, 621-633 (2020).

[25] Menazea A. A., Ezzat H. A., Omara W., Basyouni O. H., Ibrahim S. A., Mohamed A. A., Tawfik W., Ibrahim M. A., Chitosan/graphene oxide composite as an effective removal of Ni, Cu, As, Cd and Pb from wastewater, 1189 ,112980, Computational and Theoretical Chemistry, (2020).

[26] Badry R., Ibrahim A., Gamal F., Shehata D., Ezzat H., Elhaes H., Ibrahim M., Electronic Properties of Polyvinyl alcohol/ TiO2/SiO2 Nanocomposites, Biointerface Research of Applied Chemistry, 10, 6427-6435,(2020).

[27] Badry R., El-Khodary S., Elhaes H., Nada N., Ibrahim M., On the Molecular Modeling Analyses of Sodium Carboxymethyl Cellulose Treated with Acetic Acid, Letters in Applied Nano BioScience, 8, 553-557(2019).

[28] Bayoumy A.M., Youssif G., Elgohary E.A., Husien S., Salah El Deen H., Albeltagy N.M., Abdelnaby D.M., Medhat A., Elhaes H., Ibrahim M.A., Impact of solvation on the geometrical parameters of some amino acids, Letters in Applied NanoBioScience, 8, 567-570(2019).

[29] Ibrahim M., Mahmoud A.A., Computational Notes on the Reactivity of Some Functional Groups, Journal of Computational and Theoretical Nanoscience, 6, 1523-1526 (2009).

[30] Omar A., Ezzat H., Elhaes H., Ibrahim M. A., Molecular Modeling Analyses for Modified Biopolymers, Biointerface Research of Applied Chemistry, 11, 7847-7859 ,(2021).

[31] Ezzat H. A., Gomaa I., Gawad A. El-D. A., Osman O., Mahmoud A. A., Sleim M., Elhaes H., Ibrahim M. A., Semiempirical Molecular Modeling Analyses for Graphene/Nickel Oxide Nanocomposite, Letters in applied NanoBioScince. 9, 1459 – 1466, (2020).

[32] Bayoumy A.M., Refaat A., Yahia I.S., Zahran H.Y., Elhaes H., Ibrahim M.A., Shkir M., Functionalization of graphene quantum dots (GQDs) with chitosan biopolymer for biophysical applications, Optical and Quantum Electronics, 52, 1-14 (2019).

[33] Refaat A., Ibrahim M.A., Elhaes H., Badry R., Ezzat H., Yahia I.S., Zahran H.Y., Shkir M., Geometrical, vibrational and physical properties of polyvinyl chloride nanocomposites: Molecular modeling approach, Journal of Theoretical and Computational Chemistry, 18, 1950037 (2019).

[34] Ezzat H.A., Hegazy M.A., Nada N.A., Ibrahim M.A., Effect of Nano Metal Oxides on the Electronic Properties of Cellulose, Chitosan and Sodium Alginate, Biointerface Research in Applied Chemistry, 9, 4143-4149 (2019).

[35] Ibrahim M., Elhaes H., Computational Spectroscopic Study of Copper, Cadmium, Lead and Zinc Interactions in the Environment, International Journal of Environment and Pollution, 23, 417-424 (2005).

[36] Politzer P., Laurence P. R., Jayasuriya K., Molecular electrostatic potentials: an effective tool for the elucidation of biochemical phenomena, Environmental Health Perspectives, 61, 191-202 (1985).

[37] Sahin, Z.S., Şenöz H., Tezcan H., Büyükgüngör O., Synthesis, spectral analysis, structural elucidation and quantum chemical studies of (E)-methyl-4-[(2-phenylhydrazono)methyl]benzoate, Spectrochimica Acta Part A: Molecular and Biomolecular Spectroscopy, 143, 91-100 (2015).

[38] Frisch M.J., Trucks G. W., Schlegel H. B., Scuseria G. E., Robb M. A., Cheeseman J. R., Scalmani G., Barone V., Mennucci B., Petersson G. A., Gaussian09, revisions D. 01 and B. 01; Gaussian, Inc. Wallingford, CT (2010).

[39] Becke A. D., Density-functional thermochemistry. III. The role of exact exchange, The Journal of Chemical Physics, 98, 5648-5652 (1993).

[40] Lee C., Yang W., Parr R.G., Development of the Colle-Salvetti correlation-energy formula into a functional of the electron density, Physical Review B, 37, 785-789 (1988).

[41] Muzaffar S., Imtiaz Sh., Ali S. M., Demonstrating accuracy of the proposed protocol for structure elucidation of cyclodextrin inclusion complexes by validation using DFT studies, Journal of Molecular Structure, 12175, 128419 (2020).

[42] Ignaczak A., Orszański Ł., Adamiak M., Olejniczak A. B., Comparative DFT study of inclusion complexes of thymidine-carborane conjugate with β-cyclodextrin and heptakis(2,6-O-dimethyl)-β-cyclodextrin in water, Journal of Molecular Liquids, 315, 113767 (2020).

[43] Badry R., Radwan S. H., Ezzat D., Ezzat H., Elhaes H., Ibrahim M., Study of the Electronic Properties of Graphene Oxide/(PANi/Teflon). Biointerface Research in Applied Chemistry, 10, 6926 – 6935(2020).

[44] Bayoumy A. M., Refaat A., Yahia I. S, Zahran H. Y., Elhaes H., Ibrahim M. A., Shkir Mohd., Functionalization of Graphene Quantum Dots (GQDs) with Chitosan Biopolymer for Biophysical Applications, Optical and Quantum Electronics, 52, 16 (2020).

[45] Miehlich B., Savin A., Stoll H., Preuss H., Results obtained with the correlation energy density functionals of becke and Lee, Yang and Parr, Chemical Physics Letters, 157, 200-206(1989).

[46] Abdelsalam H., Elhaes H., Ibrahim M.A., Tuning electronic properties in graphene quantum dots by chemical functionalization: Density functional theory calculations, Chemical Physics Letters, 695, 138-148 (2018).

[47] Abdelsalam H., Saroka V.A., Ali M., Teleb N.H., Elhaes H., Ibrahim M.A., Stability and electronic properties of edge functionalized silicene quantum dots: A first principles study, Physica E: Low-dimensional Systems and Nanostructures, 108, 339–346 (2019).

[48] Abdelsalam H., Elhaes H., Ibrahim M. A., First principles study of edge carboxylated graphene quantum dots, Physica B, 537, 77-86 (2018).

[49] Hansch C., Leo L., Exploring QSAR: fundamentals and applications in chemistry and biology, American Chemical Society, Washington (1995)

[50] Welsh W. J., Tong W., Georgopoulos PG Toxicoinformatics: an introduction in: computational toxicology: risk assessment for pharmaceutical and environmental chemicals. In: Ekins S (ed) John Wiley & Sons, Inc., New Jersey, 151–181(2007).

[51] Elhaes H., Osman O., Ibrahim M., Interaction of nano structure material with heme molecule: modelling approach, Journal of Computational and Theoretical Nanoscience, 9, 901–905 (2012).